Acta. Chim. Asiana., 2024, 7(2), 449-463
e-ISSN/p-ISSN 2550-0503/2550-049x
Available online at: www.aca.unram.ac.id

RESEARCH PAPER

Aqueous phase synthesis of 2-D copper nanosheets stabilized by organic moieties with enhanced photocatalytic and biological activity.

Asma Sohail[*a],Widya Fatriasari[b], Sobia Zia[c], Shahnaz[a], Shagufta Irshad[c]

[a] Department of Chemistry, Lahore College for Women University, Lahore 54000, Pakistan.
[b] Research Center for Biomass and Bioproducts, National Research and Innovation Agency BRIN, Jl Raya Bogor KM 46, Cibinong, 16911, Indonesia
[c] Department of Chemistry, Government Graduate College for Women, Gulberg, Lahore, Pakistan
[*]E-mail: asmasohail4694@gmail.com

DOI: 10.29303/aca.v7i2.211

Article info:

Received 22/07/2024

Revised 18/09/2024

Accepted 24/09/2024

Available online 30/10/2024

Abstract: Copper nanosheets supported by organic ligands are significant for biological, electrical, and catalytic applications. The discovery that the coronavirus has a significantly reduced maximum survival period on copper surfaces has elevated the utility of copper nanomaterials. Here, we report a non-hazardous and inexpensive biological technique for forming copper nanosheets (Cu Nsts); synthesis of Cu Nsts has always been a challenge for researchers due to the significant problem of oxidation; in this research, we have successfully synthesized stable Cu Nsts by using *Saussurea lappa* root extract for the first time, the obtained Cu Nsts has a shiny black color with self-standing ability, the crystal structure of Cu nanosheets was determined using Powder X-ray diffraction (PXRD), Scanning electron microscopy (SEM) revealed that copper nanoparticles grow and aggregates to form Cu Nsts. The surface morphology of Cu Nsts is clear evidence of their synthesis. These nanosheets were very proficient in the deduction of harmful dye (methylene blue); within 105 minutes, the degradation capacity of Cu nanosheets for methylene blue reached 93.493%. This remarkable property of Cu Nsts as a photocatalyst gives potential application for removing dyes from industrial wastewater. Cu Nsts showed excellent antioxidant and antibacterial activity. The Cu Nsts demonstrated potent inhibitory zones against E. coli, with inhibition zones measuring 39 mm. This research lays the foundations for purifying wastewater from harmful dyes and bacteria.

Keywords: Copper nanosheets; Photocatalytic; Antioxidant activity; Organic moieties, antibacterial, *Saussurea lappa*

Citation: Sohail, A., Fatriasari, W. ., Zia, S. ., Shahnaz, & Irshad , S. (2024), Aqueous phase synthesis of 2-D copper nanosheets stabilized by organic moieties with enhanced photocatalytic and biological activity. *Acta Chimica Asiana*, 7(2), 449–463. https://doi.org/10.29303/aca.v7i2.211

INTRODUCTION

Our world has transformed into a marvelous technological sphere in which every day is a miracle. One of these wonders is the magnificent discovery of nanomaterials, which paved the corridor to the creation of fabulous gadgets, instruments, medicines, devices, and many other valuable things [1]. Green synthesis is an eco-accommodating strategy for assembling much-described nanostructures [2]. Most of the surveys found that nanomaterials synthesized by plants are more stable than those synthesized by microorganisms. Green principle-based synthesized nanostructures are known to take on diverse applications in the study of biology and medicine compared to the nanostructures synthesized by chemical protocols, which require the usage of harmful solvents or surfactants [3]. Cu nanoparticles are unique in contrast to other metal nanostructures because of their excellent photocatalytic, electrical, thermal, and visual properties, and therefore, they can be utilized as catalysts and sensors [4]. Nanosheets are a potential nanomaterial because of their nanoscale thickness, in-plane network, and holes between interface regions [5]. Cu

nanostructures have engrossed many researchers because they are cheaper than gold and silver nanostructures [6] and utilized in conductive inks, catalysis, and cooling fluids [7]. Inkjet printing is the fittest innovation that uses expensive metals, such as Au and Ag, to print exceptionally conductive components. The expenses of these metals are incredibly high. In this way, Copper is, for the most part, favored for creating profoundly conductive Cu designs on a plastic substrate by inkjet printing in light of its high conductivity and low price [8]. Copper nanostructures are thought to be very sensitive to Gram-negative and Gram-positive bacteria. They have a lot of potential as biocidal and antimicrobial agents [9].

Saussurea lappa (*S. lappa*) is often referred to as Costus. It is a tall, perennial herb that is aromatic and therapeutic, growing to a height of 1-2 meters [10]. *S. lappa* is native to Asia's cold, temperate, and arctic climates. It has been tested for various pharmacological effects and has demonstrated hepatoprotective, anti-tumor, anti-convulsant, and anti-angiogenic effects [11]. For decades, dried *S. lappa* roots have been used to cure various illnesses and conditions, including rheumatism, pulmonary diseases, inflammation, stomach disorders, and bronchitis [12]. This plant may be employed to produce antiviral solid medications [13]. Additionally, *S. lappa* extracts can treat some infections in place of antibiotics and help protect people against various diseases [14]. Figure 1 shows physical appearance of *Saussurea lappa.*

Dyes are toxic chemical compounds that cause the death of marine life [15]. Removal of these dyes is needed to guarantee a protected and clean ecosystem. Elimination of these toxic dyes is not easy because they have a very complex structure. A photocatalytic property of nanoparticles that uses sunlight provides a proficient way to remove dye completely from water [16]. Methylene blue (MB) is a common azo dye used for photocatalytic studies due to its stability, solubility in water, and non-biodegradability. Numerous health concerns could result from releasing wastewater contaminated with MB from enterprises. In particular, MB dye can cause several diseases in humans, including cyanosis, necrosis of the tissues, nausea, yellowing of the skin, and heart problems [17]. Additionally, the presence of MB has become a significant concern for plants since it can limit growth and reduce pigment [18]. Degradation of dye using sunlight is a fairly greener methodology when contrasted with UV light [19]. Copper nanostructures act as the most significant nanocatalyst for eliminating these dyes. Other nanostructures, such as ZnO and TiO_2, are also used to remove these dyes, but these nanostructures need a shorter wavelength of light to eliminate dyes [20]. Therefore, we can predict that copper nanostructures can be efficiently used for cleaning water.

Unfortunately, the resources needed to make 2-D Copper nanosheets are limited. Furthermore, the manufacture of 2-D Copper nanosheets (Cu Nsts) necessitates using hazardous substances such as ammonia and N_2H_4, as well as sophisticated techniques [21]. To the best of our knowledge, no single-step synthesis of Cu Nsts utilizing an aqueous extract of *Saussurea lappa* root has been reported before. In the present study, we have successfully synthesized Cu Nsts by a one-pot, eco-sustainable technique from *Saussurea lappa* root extract as a reducing agent and tested the efficiency of Cu Nsts for photocatalytic degradation of methylene blue (MB). The antibacterial activity of Cu Nsts was also assessed against Escherichia coli (E. coli). [4], gaseous, and solid.

MATERIALS AND METHODS

Materials

Copper sulfate pentahydrate (6.24g, 0.1M), 2,2-diphenyl-1-picrylhydrazyl (DPPH) (4 mg, 0.1mM), Methylene Blue (MB) dye (0.095g, 10^{-3} M), ethanol (100 mL), gallic acid. The root of *Saussurea lappa* Clarke (Compositae) used in this study was purchased from a local herbal store in Bedian Road, Lahore, Pakistan. Roots were dried and ground into a fine powder.

Figure 1. Digital photograph of Saussurea lappa root

Phytochemical analysis

Phytochemical analysis of a crude extract of *Saussurea lappa* root and the remaining extract of Cu Nsts synthesis was done using standard procedures [22].

Synthesis of Copper Nanoparticles

To prepare Cu Nsts, 180 ml of a fresh extract of *Saussurea lappa* root was mixed homogeneously with 240 ml of 0.1 M Copper sulfate pentahydrate solution; a rapid color change was observed, which indicated the redox reaction occurred. The mixture was then allowed to stand, and the reddish-brown suspension of Cu nanostructures was settled at the bottom of the flask after six hours. The reaction mixture was then centrifuged at 4000 rpm for twenty minutes, and the obtained Cu Nsts were washed thrice with distilled water to remove any unreacted reagents and allowed to dry at 60°C. These Nsts were then calcined at 300°C for 1 hour [23].

Characterization of copper nanosheets

UV–Visible spectroscopy analysis was done to monitor the progress of the reaction by using a Halo DB-20 UV / Visible Double Beam Spectrophotometer by taking an aqueous extract of *Saussurea lappa* root as blank, after the reaction was completed; the reaction mixture was centrifuged at 4,000 rpm for 20 minutes to remove incoherent phytochemicals. The solid substance was then suspended in de-ionized water and scanned at 200 to 800 nm wavelengths. Attenuated total reflection-Fourier transform infrared Spectroscopy (ATR-FTIR) was done by using IRT racer-100 Shimadzu Diamond ATR, and Powder X-ray diffraction analysis (PXRD) was used to determine the phase, crystal structures, and lattice parameters of synthesized nanosheets. PXRD analysis was done by using a Powder X-ray diffractometer (Bruker D8 Discover) with Cu-kα radiation source, and scanning electron microscopy (SEM) analysis was done to determine the surface morphology of synthesized Cu Nsts by using FEI Nova 450 NanoSEM.

Antibacterial Activity

This study used a gram-negative bacterial strain of Escherichia coli. A nutrient broth solution (0.5 g in 50 ml double-distilled water) was prepared in a flask. The conical flask was sealed and autoclaved for twenty minutes at 15 lb./sq. Inch pressure at 121°C. After that, 1 mL of bacterium strain was cooled to ambient temperature, poured into a flask, and placed in a shaking incubator for 24 hours. After 24 hours, the bacteria culture was used as an inoculum for antibacterial screening. The agar solution was made by dissolving 1.3 gm of nutrient agar in 50 ml of distilled water and sterilizing by autoclaving at 121°C for 20 minutes at 15 lb./sq. Inch pressure. A small quantity of bacterial culture was added to the agar solution after it had cooled to room temperature.

The bacteria, standard antibiotic (Levofloxacin), and solvent used were all marked on the sterilized Petri plate. Nutritional agar was poured into this sterilized Petri plate at a temperature of 44°C. After pouring the medium into the dish, let it cool to room temperature. To form wells on the agar plate, a sterile polystyrene tip (4 mm) was utilized. The antibacterial activity was measured by the diameter of the zone of inhibition surrounding the wells.

Photocatalytic action

The photocatalytic action of Cu Nsts was assessed by utilizing the aqueous solution of Methylene Blue (MB) dye; 15 mg of Cu Nsts were dispersed in 300 ml of 10^{-3} M solution of methylene blue dye. `The solution was left for a half-hour in the dark with continuous stirring. Then, the solution was uncovered to sunshine. A control reaction (without copper nanosheets) was also kept running simultaneously. After every fifteen minutes, 3 ml of suspension was taken from the solution and centrifuged. The reaction rate was analyzed using UV-visible spectroscopy; the following equation was used to calculate the degradation percentage.

$$D = \frac{Ao - A}{Ao} X\ 100$$

Antioxidant activity

DPPH free radical assay was used to determine the antioxidant activity of Cu Nsts. In 2.9 ml of a solution (10 mg/ml) of Cu Nsts, 100 microliters of 0.1mM DPPH solution were added. Then, the solution was left in the dark at 32°C for 25 minutes. Following 25 minutes, the absorbance of the solution was taken. DPPH was taken as control. The equation below is used to calculate the percentage of antioxidant activity.

$$\%\ RSA = \frac{Abs\ control - Abs\ sample}{Abs\ control} X\ 100$$

The decrease in the absorption of the DPPH solution after the addition of an antioxidant was measured at 517nm. Gallic acid was used as a reference.

RESULTS AND DISCUSSION

The identification of phytochemicals in *Saussurea lappa* root aqueous extract and a supernatant layer of Cu Nsts indicated the existence of many biologically active

compounds, as presented in Table 1. The metallic nanosheets are thought to be formed by the reduction of metal ions reduced by these natural compounds, particularly phenols [24].

Analysis of Copper nanosheets biosynthetic pathway

Copper nanosheets are synthesized using *Saussurea lappa* (*S. lappa*) root extract, a straightforward, ecologically friendly, and fast process. After mixing *Saussurea lappa* root extract and 0.1 M Copper sulfate pentahydrate solution, the color changed from light blue to bottle green after 15 minutes and to olive green after 30 minutes, indicating Cu Nsts' formation. Colour change of reaction mixture is shown in Figure 2. A saturated solution of Copper sulfate contains Cu^{2+} and SO_4^{2-} ions. The action of phytochemicals found in the *S. lappa* root extract causes the reduction of Cu^{2+}, such as *S. lappa* contains polyphenols that attach to Cu^{2+} ions to form metal complexes, which reduces Cu^{2+} to Cu.

The metallic copper nuclei then begin to develop into nanosheets as shown in Figre 2. Various biomolecules from S. lappa root extract stabilized copper nanosheets. Due to its insolubility in water, Cu Nsts begin to precipitate. During washing with distilled water and ethanol, unreacted phytochemicals stuck to the surface of nanostructures were eliminated, yielding self-standing shiny black crystalline Cu Nsts.

Table 1. Results of phytochemical analysis.

Test	*S.lappa* root extract	A supernatant layer of Cu Nsts
Wagner's test	(++++)	(++)
Hager's test	(++++)	(++)
For anthocyanins	(-)	(-)
For carbohydrates (Molisch's test)	(++++)	(-)
Fehling test for reducing sugar	(++++)	(++++)
Iodine test	(-)	(-)
Test for steroid	(++)	(-)
Test for flavonoids (Alkaline reagent test)	(++++)	(-)
Test for phytosterol (Salkowski's test)	(++++)	(++)
Test for saponins	(++++)	(++)

Note: (++++) shows the maximum presence, (++) shows the minimum presence, and (-) shows absence.

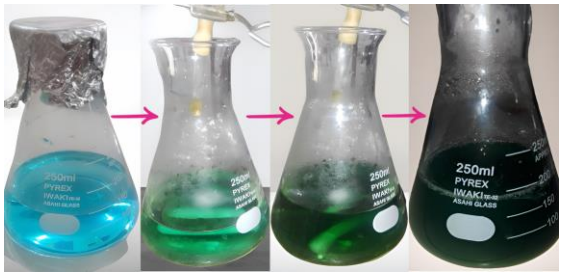

Figure 2. Color changes during the reaction between S. lappa root extract and Copper sulfate pentahydrate solution

Figure 3. Digital photograph of Copper nanosheets synthesized using *S. lappa* root extract

UV–visible spectroscopic studies

Cu Nsts were characterized using a UV-visible spectrophotometer; the results are shown in Figure 4. UV Visible Spectroscopy is a quick and sensitive tool for detecting nanostructure formation and stability. Clear evidence of the peak of Cu Nsts in the 550–600 nm range, demonstrating Cu Nsts production; the maximum absorbance of Cu Nsts was observed at 581 nm [25].

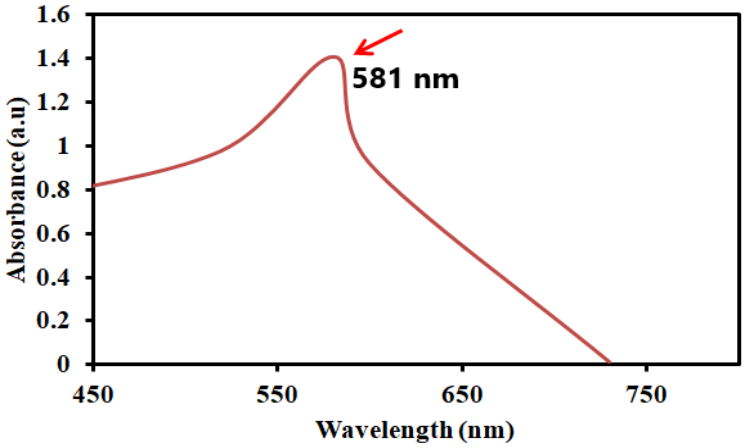

Figure 4. Represents the absorbance of Cu Nsts after 24 hrs. Cu Nsts showed absorbance at 581 nm

ATR-FTIR analysis

Cu Nsts were analyzed using FTIR to determine the capping and reducing agents. ATR- FTIR spectra of synthesized Cu Nsts from *S. lappa* root extract are shown in Figure 5. The ATR- FTIR result of Cu Nsts showed a peak absorption peak at 1033.85 $cm^{-1,}$ indicating C-O stretching in phenol. The peak at 1620.21 cm^{-1} represents C=N stretching in oximes, and the peak at 1867.09 cm^{-1} corresponds to the C=O stretch in cyclic, 5-membered anhydrides. The peak at 2931.81 cm^{-1} corresponds to the C– H stretching in the Ac–H bond in aldehydes. The peak at 3259 cm^{-1} represents O–H in alcohol. ATR-FTIR spectrum of Cu Nsts recommended that Cu Nsts contain different organic molecules such as esters, aldehydes, oximes, phenols, and anhydrides.

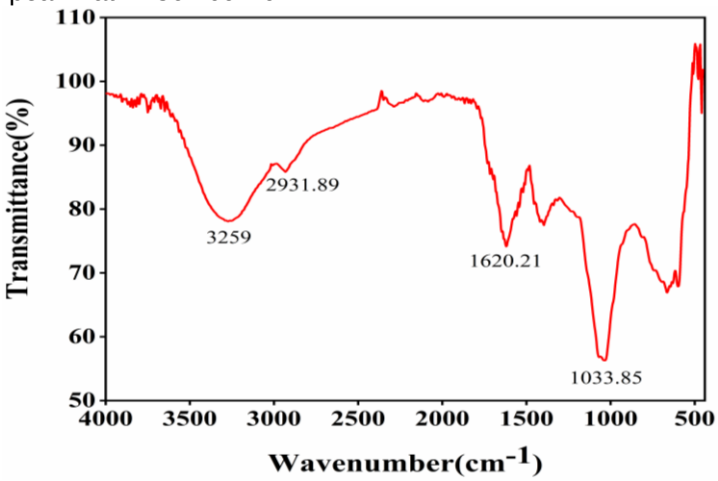

Figure 5. FTIR spectrum of Cu Nsts

SEM analysis

A scanning electron microscope was utilized to carry out the morphological analysis of Cu Nsts. The patterns and foldings of Cu Nsts are seen in Figure 6. This result proved the formation of two-dimensional nanosheets of copper. The thickness and width of the nanosheets were also calculated using ImageJ software; the obtained Cu Nsts have a thickness of 747 nm.

The current method could aid in the production of symmetric nanosheets. The SEM image of stabilized Cu Nsts indicated that the nanosheets of small size were clustered and aggregated and formed larger nanosheets. Small fragments of nanosheets can also be seen. The present results of SEM are in acceptable concurrence with published literature [26]. SEM images show that the width of nanosheets ranges from 400 nm to 1200 nm with an average width of 748.7 nm as shown in Figure 7; furthermore, SEM image depicts the interesting layered architecture of Cu Nsts fabrication with different stacking orientations. In addition, the availability of polyphenols (from components of *S.lappa* extract) is ascribed to the size variation of Cu Nsts, which have significant forces of attraction

between particles. The prevalence of hydrogen-bonded molecules containing various phenolic ligands contributes to the production of agglomerates [27].

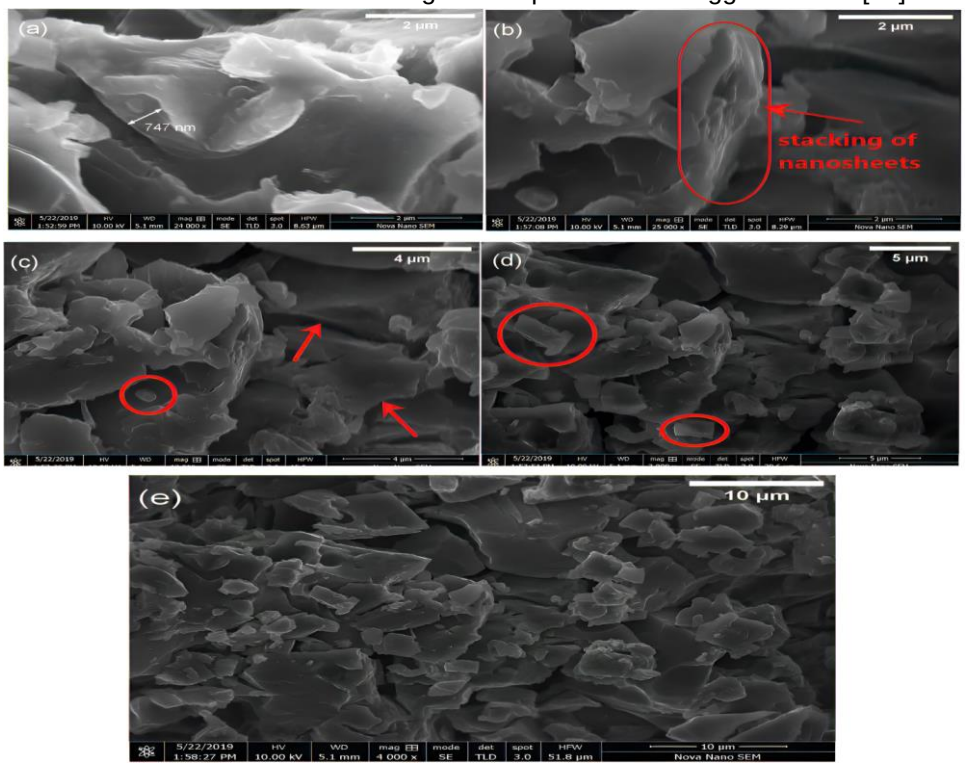

Figure 6. Represented the SEM images of Cu Nsts

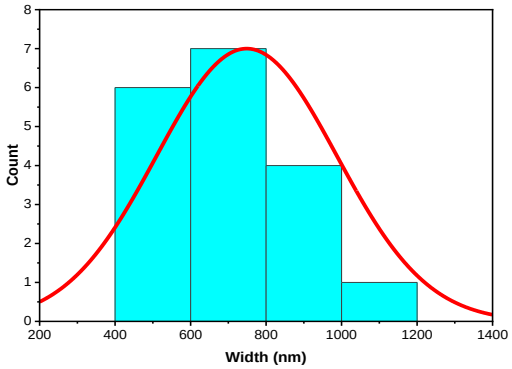

Figure 7. Width distribution histogram for Cu Nsts

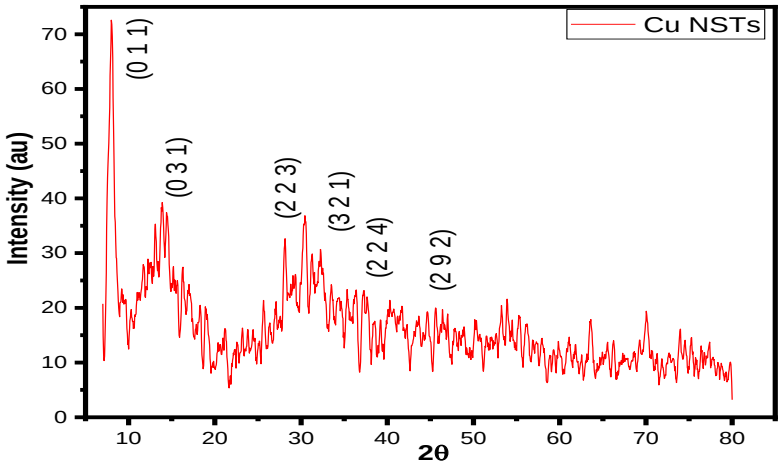

Figure 8. PXRD pattern of Cu Nsts, showing major diffraction peaks

PXRD Analysis of Synthesized Cu Nsts

The distinctive peaks found in the XRD pattern were used to analyze the crystal structure of Cu Nsts. Peaks in the Cu Nsts spectra occurred with diffraction angles ranging from 7 to 80 with a step size 0.05 as shown in Figure 8. 2θ and h k l values are given in Table 2. The XRD findings revealed that green synthesized Cu Nsts have a single-phase and an orthorhombic structure.

Table 2. PXRD values.

2θ	d-spacing [Å]	h k l value
8.005418	11.04437	0 1 1
14.531850	6.09558	0 3 1
16.117730	5.49921	0 2 2
21.352790	4.16134	2 0 1
30.082900	2.97065	2 2 3
32.454900	2.75875	3 2 1
35.289880	2.54336	2 2 4
46.54865	1.95108	2 9 2

The Rietveld refinement was done with the X'Pert High Score Plus software. The Rietveld fitting strategy is simple in concept. It refines the crystal parameters of the computed pattern using the least-squares technique until it fits the measured XRD data. For determining accurate crystal properties of a material, successful Rietveld refinement is necessary [28]. XRD profile elements such as intensity, FWHM, d-spacing, and position determine the crystallographic properties of materials [29]. As a result, it is essential to consider such values during the refinement process. The peak location significantly correlates to the lattice parameters regarding crystalline properties, and their correlation follows Bragg's rule [30]. Furthermore, the width indicates the crystallite size, while the peak intensity demonstrates the phase weight fraction [31]. The XRD pattern reveals that measured and estimated statistical data are well-matched, and all experimental peaks are allowed Bragg position (2Ɵ), with a space group of space group P n m a (62). The goodness of fit (γ^2 = 1.61), R (expected) = 16.1, R (profile) = 16.4, R (weighted profile) = 20.5, and Bragg factor (RB = 6.92) were used to assess the data's fitting quality. The refining was done using the crystallographic open database's CIF file no. 4120102. The dataset of the phase, the unit cell, and the x and z atomic coordinates were the specific parameters for the improved phase. These parameters generated tentative structural designs for the Cu Nsts crystal. The value of γ^2 should be close to two but not below one. γ^2<1 indicates that the standard uncertainties have been exaggerated or that the model has been fitted with a large number of parameters. Furthermore, γ^2 >> 1 demonstrates that typical uncertainties are understated, implying that the model is inadequate or incorrect. Our rietveld refined value of γ^2 is in satisfactory correlation to the accepted ones, indicating that the diffraction data of Cu Nsts samples were well refined [32]. Rietveld refinement parameters are given in Table 2 and crystalline structure of Cu Nsts at is shown in Figure 9 and Figure 10. drawn by visualization for electronic and structural analysis (VESTA) software. Figure 11 shows 3-D map for XRD pattern of Cu Nsts drawn by X'Pert High Score Plus software.

Photocatalytic degradation of Methylene blue

Methylene blue displays a strong absorption maximum at 664 nm. When the solution of MB dye-containing Cu Nsts is exposed to UV or near UV irradiation, Sunlight photons confront the surfaces of Cu Nsts and activate electrons. The catalyst became highly active, creating free electrons and holes on the catalyst's surface. Active O^{2-}, HOO, and HO free radicals were generated from the oxygen dissolved in the reaction medium. It has been discovered that these radicals are extraordinarily reactive, transforming extremely complex organic dye molecules into simpler organic compounds, hence aiding dye removal. When exposed to sunlight, these bioactive Cu Nsts could be used as a potent and durable photocatalyst for MB dye degradation [33]. The schematic mechanism of Cu Nst is shown in Figure 12.

Figure 12 shows the results of the photocatalytic activity of MB dye degradation. The photocatalytic efficiency of synthesized Cu Nsts employing *S. lappa* root extract was outstanding for dye removal. Degradation of dye does not occur instantly. Degradation of dye was examined by observing the changes in the UV spectrum of a solution. It was noted that the absorption peak of methylene blue was decreasing with the increase in time and came to its lowest value. The absorption peaks corresponding to methylene blue showed slow degradation initially, but after 20 minutes, it showed rapid degradation. The process of degradation again slowed at 105 minutes, and the degradation potential of the green synthesized Cu Nsts for methylene blue reached 93.493 % after 105 minutes. Reaction of Cu Nsts with methylene blue is shown in Figure 13. Degradation of methylene blue dye with respect to time is shown in Figure 14.

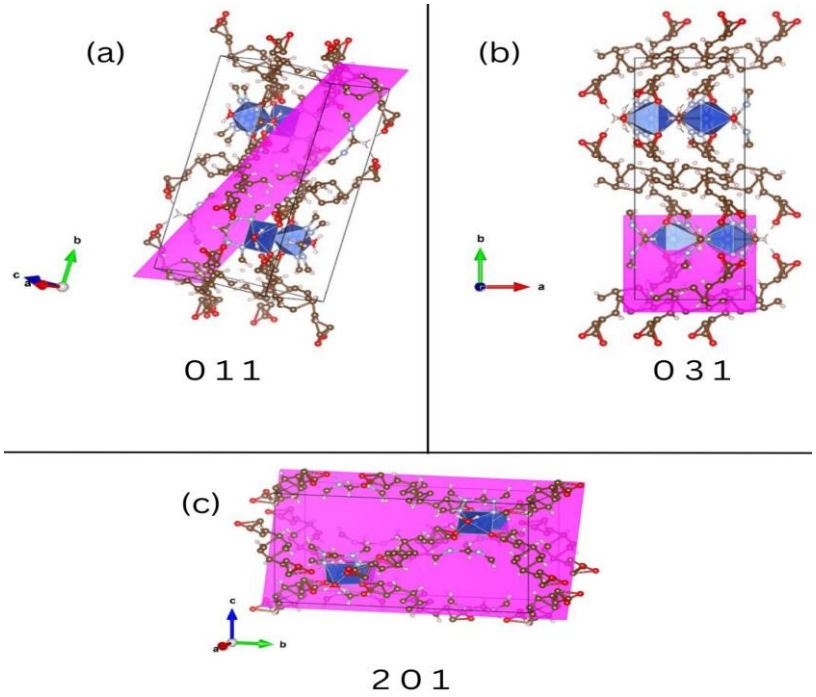

Figure 9. Crystalline structural representation of Cu Nsts at different planes

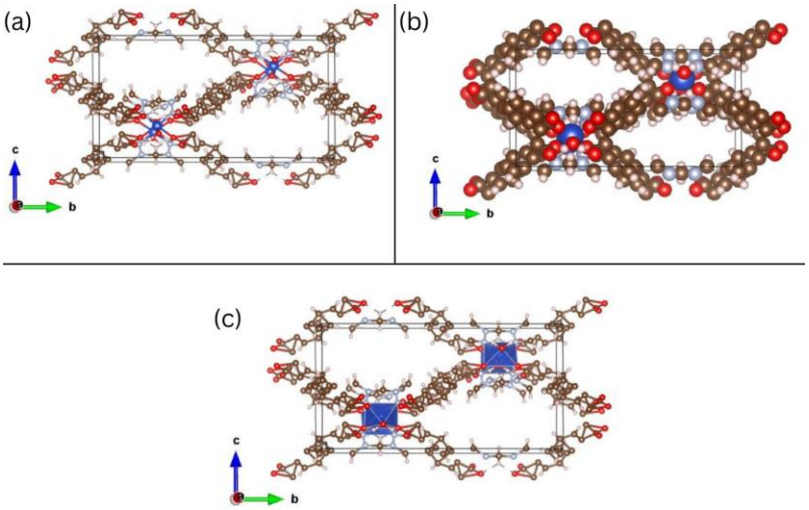

Figure 10. Crystalline structural representation of Cu Nsts (a) Ball and Stick model, (b) Space-fill model, (c) polyhedral model

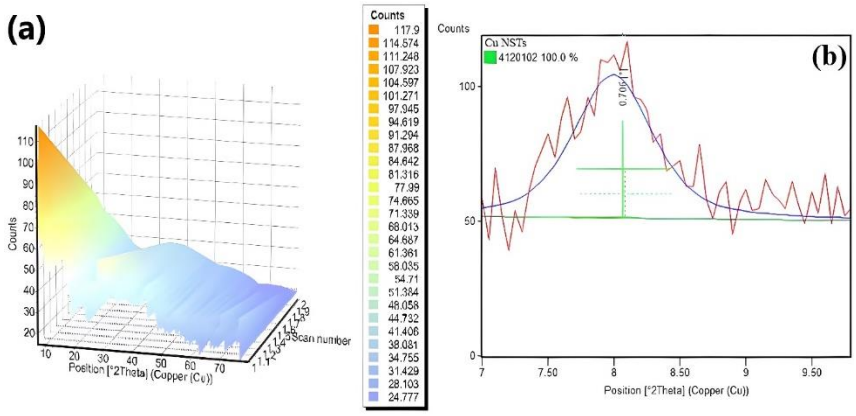

Figure 11. (a) 3-D map for XRD pattern of Cu Nsts, (b) FWHM-based Rietveld refinement for Cu Nsts

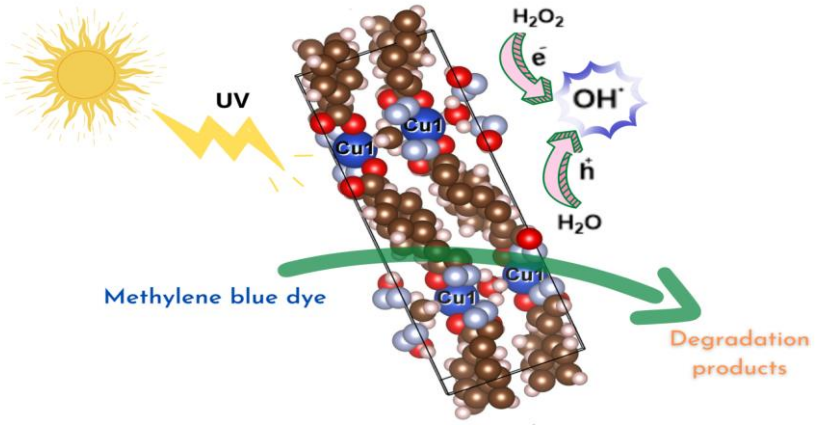

Figure 12. A proposed mechanism for photoc atalytic activity of Cu Nsts

The kinetics of dye degradation was characterized by an early slow phase accompanied by a faster secondary phase. In the advanced stage of photocatalysis, the rapid dye removal efficiency was aided by the abundance of catalytic sites and a greater relative concentration. The tertiary phase progressed at a modest rate due to a decrease in the active sites of the photocatalyst.

Table 3. The Rietveld refinement parameters of Cu Nsts.

Parameters	value
Quantitative analysis (phase 1)	100%
Lattice parameters (Å)	a=8.3, b=23, c= 11.9
unit cell volume (Å3)	2271.7
density (g/cm3)	1.38
Crystallite size (Å)	91.4

The following equations investigated the kinetics of photocatalytic dye degradation by the catalyst in zero-order and first-order.

$$A_o - A = k_o t$$

$$\ln(A_o/A) = k_1 t$$

where A_0 is the initial dye absorbance, and A is the dye absorbance at time t. The zero-order and first-orde r rate constants are k_0 and k_1[34].

Absorption and percentage of degradation of methylene blue dye is shown in Figure 15. The suggested approach for Cu Nsts biosynthesis using *S. lappa* root extract has a short process time and temperature, resulting in Cu Nsts with high photocatalytic activity. Figure 16 compares the catalytic potential Cu Nsts' with those reported catalysts for reducing MB. The different phytochemicals found in the *S. lappa* root extract have a rapid and significant bioreduction activity, allowing for the synthesis of Cu Nsts with minimal reaction time and temperature [35]. Figure 16 shows the kinetic studies of degradation of methylene blue dye, the graphs were drawn by using Origin software.

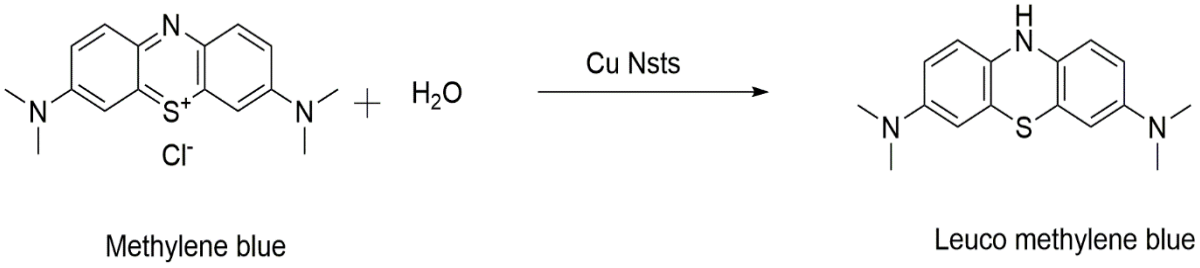

Figure 13. Reaction of methylene blue with Cu Nsts

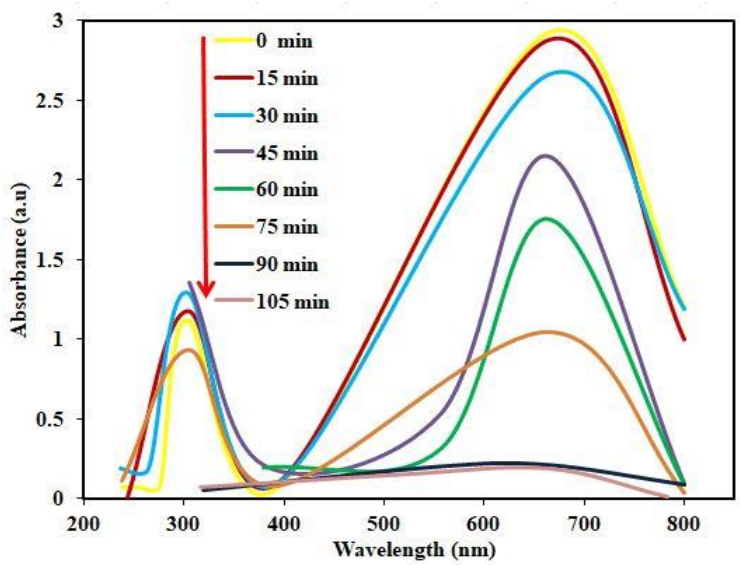

Figure 14. UV–Vis absorption of MB dye at different time intervals

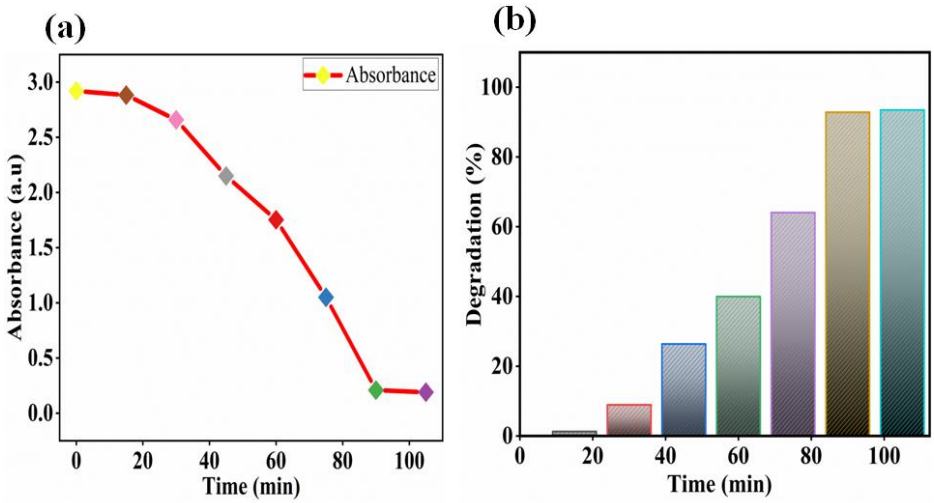

Figure 15. (a) Decrease in the absorption of methylene blue with time, (b) Percentage of degradation of methylene blue

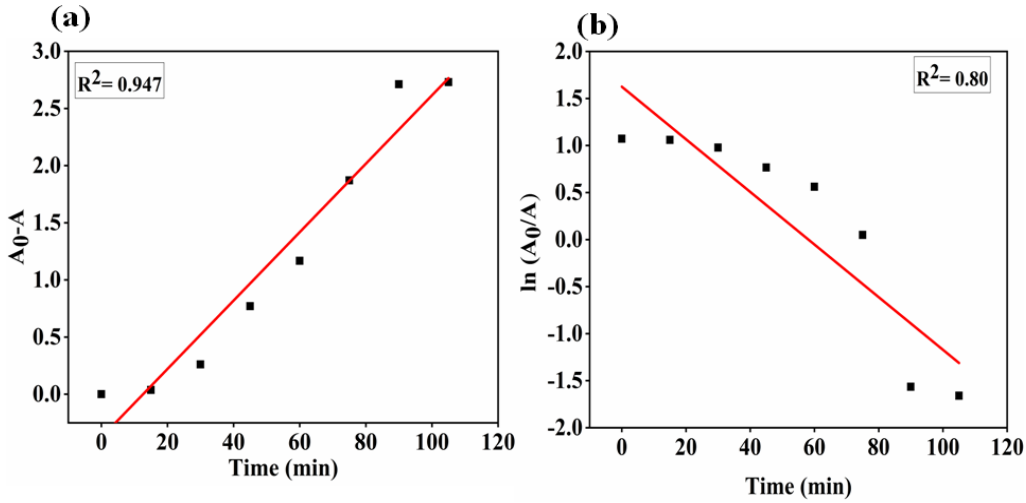

Figure 16. Degradation of methylene blue following (a) zero-order reaction, (b) first-order reaction

Table 4. Comparison of the Cu Nsts' catalytic potential with those reported catalysts for reducing MB.

Catalyst	Time (min)	MB degradation (%)	Reference
Cu Nsts	105	93.493 %	This work
Spherical-shaped magnetite nanoparticle	210	93.4	[36]
Ag/ZnO nanocomposite	120	76	[37]
ZnO/ biochar nanocomposites	225	95.19	[38]
Cobalt oxide nanoparticles	300	88%	[39]
Silver nanoparticles	150	97.57	[40]
PCN-250(Fe_2Mn)	300	100	[41]
Alginate-TiO_2	540	24.9	[42]
Nd–Gd co-doped ZnO	120	93	[43]
Commercial TiO_2 (P25)	120	81.8	[44]

Biological activity of Cu Nsts

Cu Nsts show great potential for antibacterial activity, making them prospective candidates for medical use. The green fabricated Cu Nsts could replace some antibiotic drugs to fight against human pathogens (bacteria) and be less expensive. Cu Nsts were tested for antibacterial activities. The agar well diffusion method was used to examine the bacterial strain of E. Coli (Gram-negative). Against E. Coli, the Cu Nsts displayed strong inhibitory zones. Cu ions have been shown to interfere with a variety of biological processes. Both amine and carboxyl groups are found in the bacterial cell wall, which has a strong affinity for copper ions. Cu Nsts may bind to bacteria's nucleic acid, disrupting the DNA helix. Table 5 demonstrates that the biosynthesized Cu Nsts had better antibacterial activity against E. coli, with inhibition zones measuring 39 mm. The Cu Nsts showed significantly improved antibacterial efficacy against the studied bacterial strains compared to traditional antibiotics.

Table 5. Results of antibacterial activity.

Sample	Zone of Inhibition (mm)
Cu Nsts	39 mm
Levofloxacin	40 mm
blank solvent (methanol)	15 mm

Antioxidants work as free radical scavengers, boosting the defense system's effectiveness and lowering the incidence of disease. However, oxidative stress arises when the balance of exogenous free radicals, such as those produced by pollution, alcohol, starvation, and smoking, shifts in favor of free radicals. This causes oxidative stress to damage critical cellular components like carbohydrates, lipids, and proteins, particularly DNA damage, as well as a variety of disorders such as neurological disorders, aging, cancer, and heart disease [45].

Plants contain unique metabolites that have been shown to serve a variety of functions. Plant-mediated nanomaterials synthesis comprises stepwise reduction followed by capping with these plant ingredients. Unfortunately, interactions of these components with metals are poorly understood, and the type of activity they might confer on nanosheets has yet to be discovered. The antioxidant activity of Cu Nsts capped with free radical scavenging plant components has been reported for the first time. Capped Cu Nsts were proven to be effective free radical scavengers. Cu Nsts showed an antioxidant activity of 69.45%. A result of antibacterial activity and antioxidant activity is shown in Figure 17.

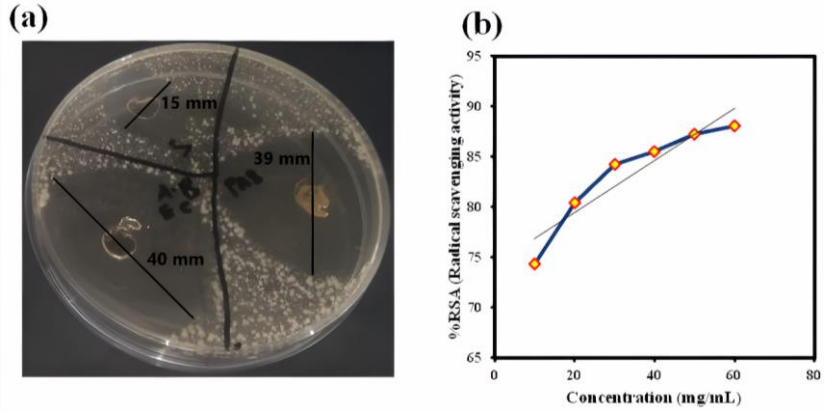

Figure 17. (a) Result of antibacterial activity, (b) Calibration curve for antioxidant activity

CONCLUSION

Copper Nsts were successfully synthesized in one pot, utilizing an aqueous extract of S. lappa under moderate circumstances. The self-assembly of synthesized Cu Nsts in the form of two-dimensional sheets having orthorhombic structure was observed. Measurements of photocatalytic activity revealed that Cu Nsts has a reasonably high degradation efficiency Against methylene blue. The nanosheets have a high bactericidal capability against bacterial infections. SEM analysis showed that the primary particles merged to yield bigger-sized secondary particles. Several thinner sheets aggregated to form nanosheet networks.

ACKNOWLEDGMENTS

The author would like to thank Saadat Anjum for her support and encouragement. She acknowledges the Department of Chemistry, Government Graduate College for Women, Gulberg, Lahore, Pakistan, and Department of Chemistry, Lahore College for Women University, Lahore, Pakistan for providing research facilities.

Declarations

Ethical approval

Not applicable

Funding

No funds, grants, or other support was received.

Availability of data and materials

Data sets generated during the current study are available from the corresponding author on reasonable request.

REFERENCES

[1] F. J. Heiligtag and M. J. M. T. Niederberger (2013) The fascinating world of nanoparticle research. *materialstoday* vol. 16, no. 7-8, pp. 262-271. https://doi.org/10.1016/j.mattod.2013.07.004

[2] S. Rajeshkumar and L. J. C.-b. i. Bharath (2017) Mechanism of plant-mediated synthesis of silver nanoparticles a review on biomolecules involved, characterisation and antibacterial activity. *Chemico-Biological Interactions* vol. 273, pp. 219-227. https://doi.org/10.1016/j.cbi.2017.06.019

[3] S. Baker, B. Harini, D. Rakshith, and S. J. J. o. P. R. Satish (2013) Marine microbes: invisible nanofactories. *Journal of Pharmacy Research* vol. 6, no. 3, pp. 383-388. https://doi.org/10.1016/j.jopr.2013.03.001

[4] M. S. Usman, M. E. El Zowalaty, K. Shameli, N. Zainuddin, M. Salama, and N. A. J. I. j. o. n. Ibrahim (2013) Synthesis, characterization, and antimicrobial properties of copper nanoparticles. *International Journal of Nanomedicinevol* 8, p. 4467. https://doi.org/10.2147/IJN.S50837

[5] M. Liu, P. A. Gurr, Q. Fu, P. A. Webley, and G. G. J. J. o. M. C. A. Qiao (2018) Two-dimensional nanosheet-based gas separation membranes. *Materials Chemistry A* vol. 6, no. 46, pp. 23169-23196. https://doi.org/10.1039/C8TA09070J

[6] P. Ananthi and S. M. J. J. I. J. I. R. S. E. T. Kala (2017) Plant extract mediated synthesis and characterization of copper nanoparticles and their pharmacological activities. *International Journal of Innovative Research in Science, Engineering and Technology*, vol. 6, pp. 13455-13465. DOI:10.15680/IJIRSET.2017.0607206

[7] A. Tamilvanan, K. Balamurugan, K. Ponappa, and B. M. J. I. J. o. N. Kumar (2014) Copper nanoparticles: synthetic strategies, properties and multifunctional application. *International Journal of Nanoscience* vol. 13, no. 02, p. 1430001. https://doi.org/10.1142/S0219581X14300016

[8] K. Madhuri, K. Elango, S. J. O. p. Ponnusankar, and E. medicine (2012) Saussurea lappa (Kuth root): review of its traditional uses, phytochemistry and pharmacology. *Oriental pharmacy and experimental medicine* vol. 12, no. 1, pp. 1-9. https://doi.org/10.1007/s13596-011-0043-1

[9] R. Suman *et al.* (2020) Sustainability of coronavirus on different surfaces. *Journal of Clinical and Experimental Hepatology* vol. 10, no. 4, pp. 386-390. https://doi.org/10.1016/j.jceh.2020.04.020

[10] A. Ali *et al.* (2021) Saussurea lappa: An Important Medicinal Plant for Treatment Different Diseases: A review. *Kufa Journal for Nursing Sciences* vol. 11, no. 1, pp. 1-8. https://doi.org/10.36321/kjns.vi20211.427

[11] K. Madhuri, K. Elango, and S. Ponnusankar (2012) Saussurea lappa (Kuth root): review of its traditional uses, phytochemistry and pharmacology. *Oriental pharmacy and Experimental*

medicine. vol. 12, pp. 1-9. https://doi.org/10.1007/s13596-011-0043-1

[12] M. M. Pandey, S. Rastogi, and A. K. S. Rawat (2007) Saussurea costus: Botanical, chemical and pharmacol ogical review of an ayurvedic medicinal plant. *Journal of ethnopharmacology* vol. 110, no. 3, pp. 379-390. https://doi.org/10.1016/j.jep.2006.12.033

[13] K. Zahara *et al.* (2014) A review of therapeutic potential of Saussurea lappa-An endangered plant from Himalaya. *Asian Pacific journal of tropical medicine* vol. 7, pp. S60-S69. https://doi.org/10.1016/S1995-7645(14)60204-2

[14] M. M. Deabes, A.-E. Fatah, I. Sally, S. H. E. Salem, and K. M. Naguib (2021) Antimicrobial activity of bioactive compounds extract from Saussurea costus against food spoilage microorganisms. *Egyptian Journal of Chemistry.* vol. 64, no. 6, pp. 2833-2843. https://doi.org/10.21608/ejchem.2021.69572.3528

[15] O. Akhavan and E. J. S. Ghaderi (2010) Cu and CuO nanoparticles immobilized by silica thin films as antibacterial materials and photocatalysts. *Surface and Coatings Technology* vol. 205, no. 1, pp. 219-223. https://doi.org/10.1016/j.surfcoat.2010.06.036

[16] [C. Tang, X. Huang, H. Wang, H. Shi, and G. J. J. o. h. m. Zhao (2020) Mechanism investigation on the enhanced photocatalytic oxidation of nonylphenol on hydrophobic TiO2 nanotubes. *Journal of Hazardous Materials* vol. 382, p. 121017. https://doi.org/10.1016/j.jhazmat.2019.121017

[17] R. Ahmad and R. Kumar (2010) Adsorption studies of hazardous malachite green onto treated ginger waste. *Journal of environmental management* vol. 91, no. 4, pp. 1032-1038. https://doi.org/10.1016/j.jenvman.2009.12.016

[18] A. K. Moorthy, B. G. Rathi, S. P. Shukla, K. Kumar, and V. S. Bharti (2021) Acute toxicity of textile dye Methylene blue on growth and metabolism of selected freshwater microalgae. *Environmental Toxicology and Pharmacology* vol. 82, p. 103552. https://doi.org/10.1016/j.etap.2020.103552

[19] T. Sinha, M. J. E. S. Ahmaruzzaman, and P. Research (2015) Green synthesis of copper nanoparticles for the efficient removal (degradation) of dye from aqueous phase. *Environ Sci Pollut Res* vol. 22, no. 24, pp. 20092-20100. https://doi.org/10.1007/s11356-015-5223-y

[20] R. A. Soomro, A. Nafady, S. T. H. Sherazi, N. H. Kalwar, M. R. Shah, and K. R. J. J. o. N. Hallam (2015) Catalytic reductive degradation of methyl orange using air resilient copper nanostructures. *Journal of Nanomaterials* vol. 2015. https://doi.org/10.1155/2015/136164

[21] S. Lee, S. Wang, C. Wern, and S. J. M. Yi (2021) The Green Synthesis of 2D Copper Nanosheets and Their Light Absorption. *Materials* vol. 14, no. 8, p. 1926. https://doi.org/10.3390/ma14081926

[22] R. Singh, K. Chahal, N. J. J. o. P. Singla, and Phytochemistry (2017) Chemical composition and pharmacological activities of Saussurea lappa: *A review. Journal of Pharmacognosy and Phytochemistry* vol. 6, pp. 1298-1308.

[23] S. Irshad *et al.* (2018) Green tea leaves mediated ZnO nanoparticles and its antimicrobial activity. *Cogent Chemistry* vol. 4, no. 1, p. 1469207. https://doi.org/10.1080/23312009.2018.1469207

[24] S. Ningaraju *et al.* (2021) Chaetomium globosum extract mediated gold nanoparticle synthesis and potent anti-inflammatory activity. *Analytical Biochemistry* vol 612, p. 113970. https://doi.org/10.1016/j.ab.2020.113970

[25] B. Kumar, S. Saha, M. Basu, and A. K. J. J. o. M. C. A. Ganguli (2013) Enhanced hydrogen/oxygen evolution and stability of nanocrystalline (4–6 nm) copper particles. *Journal of Materials Chemistry A* vol. 1, no. 15, pp. 4728-4735. https://doi.org/10.1039/C3TA01194A

[26] S. Muthu and M. B. J. M. T. P. Sridharan (2018) Synthesis and characterization of two dimensional copper selenide (CuSe) Nanosheets. *Materials Today Proceedings* vol. 5, no. 11, pp. 23161-23168. https://doi.org/10.1016/j.matpr.2018.11.047

[27] R. Khani, B. Roostaei, G. Bagherzade, and M. J. J. o. M. L. Moudi (2018) Green synthesis of copper nanoparticles by fruit extract of Ziziphus spina-christi (L.) Willd.: Application for adsorption of triphenylmethane dye and antibacterial assay. *Journal of Molecular Liquids* vol. 255, pp. 541-549. https://doi.org/10.1016/j.molliq.2018.02.010

[28] [S. Pratapa *et al.* (2010)XRD line-broadening characteristics of M-oxides

(M= Mg, Mg-Al, Y, Fe) nanoparticles produced by coprecipitation method. *AIP Conference Proceedings.* vol. 1284, no. 1, pp. 125-128: American Institute of Physics. https://doi.org/10.1063/1.3515533

[29] H. J. A. C. Rietveld (1967) Line profiles of neutron powder-diffraction peaks for structure refinement. *Acta Cryst* vol. 22, no. 1, pp. 151-152. https://doi.org/10.1107/S0365110X67000234

[30] H. M. J. J. o. a. C. Rietveld (1969) A profile refinement method for nuclear and magnetic structures. *J. Appl. Cryst* vol. 2, no. 2, pp. 65-71. https://doi.org/10.1107/S0021889869006558

[31] N. Hidayat, A. Hidayat, S. Hidayat, N. Mufti, A. Taufiq, and H. Heriyanto (2020) Assessing Rietveld refinement results on silicon carbide nanoparticles produced by magnesiothermal treatment. *Journal of Physics: Conference Series* vol. 1595, no. 1, p. 012032: IOP Publishing. doi:10.1088/1742-6596/1595/1/012032

[32] S. Atiq *et al.* (2017) Synthesis and investigation of structural, morphological, magnetic, dielectric and impedance spectroscopic characteristics of Ni-Zn ferrite nanoparticles. *Ceramics International* vol. 43, no. 2, pp. 2486-2494. https://doi.org/10.1016/j.ceramint.2016.11.046

[33] H. Sadiq *et al.* (2021) Green synthesis of ZnO nanoparticles from Syzygium Cumini leaves extract with robust photocatalysis applications. *Journal of Molecular Liquids* vol. 335, p. 116567. https://doi.org/10.1016/j.molliq.2021.116567

[34] N. Khorshidi, S. Khorrami, M. Olya, and F. J. O. J. C. Mottiee (2016) Photodegradation of basic dyes using nanocomposite (silver zinc oxide-copper oxide) and kinetic studies. *Oriental journal of chemistry* vol. 32, pp. 1205-1214. http://dx.doi.org/10.13005/ojc/320247

[35] K. Rambabu, G. Bharath, F. Banat, and P. L. J. J. o. h. m. Show (2021) Green synthesis of zinc oxide nanoparticles using Phoenix dactylifera waste as bioreductant for effective dye degradation and antibacterial performance in wastewater treatment. *Journal of Hazardous Materials* vol. 402, p. 123560. https://doi.org/10.1016/j.jhazmat.2020.123560

[36] T. de Oliveira Guidolin *et al.* (2021) Photocatalytic pathway on the degradation of methylene blue from aqueous solutions using magnetite nanoparticles. *Journal of Cleaner Production* vol. 318, p. 128556. https://doi.org/10.1016/j.jclepro.2021.128556

[37] M. A. Messih, M. Ahmed, A. Soltan, and S. S. Anis (2019) Synthesis and characterization of novel Ag/ZnO nanoparticles for photocatalytic degradation of methylene blue under UV and solar i rradiation. *Journal of Physics and Chemistry of Solids* vol. 135, p. 109086. https://doi.org/10.1016/j.jpcs.2019.109086

[38] F. Yu *et al.* (2021) ZnO/biochar nanocomposites via solvent free ball milling for enhanced adsorption and photocatalytic degradation of methylene blue. *Journal of Hazardous Materials* vol. 415, p. 125511. https://doi.org/10.1016/j.jhazmat.2021.125511

[39] R. Vinayagam *et al.* (2023) Green synthesized cobalt oxide nanoparticles with photocatalytic activity towards dye removal. *Environmental Research* vol. 216, p. 114766. https://doi.org/10.1016/j.envres.2022.114766

[40] J. Kadam, P. Dhawal, S. Barve, and S. Kakodkar (2020) Green synthesis of silver nanoparticles using cauliflower waste and their multifaceted applications in photocatalytic degradation of methylene blue dye and Hg^{2+} biosensing. *SN Applied Science* vol. 2, pp. 1-16. https://doi.org/10.1007/s42452-020-2543-4

[41] A. Kirchon, P. Zhang, J. Li, E. A. Joseph, W. Chen, and H.-C. Zhou (2020) Effect of isomorphic metal substitution on the fenton and photo-fenton degradation of methylene blue using Fe-based metal–organic frameworks. *ACS applied materials & interfaces* vol. 12, no. 8, pp. 9292-9299. https://doi.org/10.1021/acsami.9b21408

[42] N. X. D. Mai, D. Park, J. Yoon, and J. Hur (2018) Comparative study of hydrogel-based recyclable photocatalysts. 463 *of Nanoscience and Nanotechnol* 18, no. 2, pp. 13[illegible]. https://doi.org/10.1166/jnn.2018.14929.

[43] J. Akhtar, M. Tahir, M. Sagir, and H. S. Bamufleh (2020) Improved photocatalytic performance of Gd and Nd co-doped ZnO nanorods for the degradation of methylene blue. *Ceramics International* vol. 46, no. 8, pp. 11955-11961.

https://doi.org/10.1016/j.ceramint.2020.01.234

[44] J. Ye, C. Chao, and J. Hong (2020) Preparation of a novel nano-TiO2 photocatalytic composite using insoluble wood flour as bio-carrier and dissolved components as accele rant. *Journal of Materials Research and Technology* vol. 9, no. 5, pp. 11255-11262. https://doi.org/10.1016/j.jmrt.2020.07.099

[45] [T. Gur, I. Meydan, H. Seckin, M. Bekmezci, and F. J. E. R. Sen (2022) Green synthesis, characterization and bioactivity of biogenic zinc oxide nanoparticles. *Environmental Research* vol. 204, p. 111897. https://doi.org/10.1016/j.envres.2021.111897